

Further Evidence for BRCA1 Communication with the Inactive X Chromosome

Daniel P. Silver,^{1,6} Stoil D. Dimitrov,^{1,6} Jean Feunteun,² Rebecca Gelman,^{1,5} Ronny Drapkin,¹ Shihua D. Lu,¹ Elena Shestakova,¹ Soundarapandian Velmurugan,¹ Nicholas DeNunzio,¹ Serban Dragomir,¹ Jessica Mar,^{1,5} Xiaoling Liu,³ Sven Rottenberg,³ Jos Jonkers,³ Shridar Ganesan,^{4,*} and David M. Livingston^{1,*}

¹ Dana-Farber Cancer Institute, Harvard Medical School, Boston, MA 02115, USA

² Laboratoire Genomes et Cancer, CNRS-Université Paris XI-Institut Gustave-Roussy, 94805 Villejuif, France

³ Division of Molecular Biology, The Netherlands Cancer Institute, 1066 CX Amsterdam, The Netherlands

⁴ The Cancer Institute of New Jersey, Robert Wood Johnson Medical School, University of Medicine and Dentistry of New Jersey, 195 Little Albany Street, New Brunswick, NJ 08903, USA

⁵ Harvard School of Public Health, Boston, MA 02115, USA

⁶ These authors contributed equally to this work.

*Correspondence: ganesash@umdnj.edu (S.G.), david_livingston@dfci.harvard.edu (D.M.L.)

DOI 10.1016/j.cell.2007.02.025

SUMMARY

BRCA1, a breast and ovarian cancer-suppressor gene, exerts tumor-suppressing functions that appear to be associated, at least in part, with its DNA repair, checkpoint, and mitotic regulatory activities. Earlier work from our laboratory also suggested an ability of *BRCA1* to communicate with the inactive X chromosome (Xi) in female somatic cells (Ganesan et al., 2002). Xiao et al. (2007) (this issue of *Cell*) have challenged this conclusion. Here we discuss recently published data from our laboratory and others and present new results that, together, provide further support for a role of *BRCA1* in the regulation of XIST concentration on Xi in somatic cells.

INTRODUCTION

The *BRCA1* gene encodes multiple protein products, the most extensively studied of which is a large, multiply phosphorylated RING and BRCT motif-containing nuclear protein, p220. p220 is an E3 ubiquitin ligase, interacts with numerous protein partners, and plays a pivotal role in multiple aspects of the processes that maintain genomic integrity. In keeping with this finding, key elements of the gene have been conserved throughout plant and metazoan evolution, suggesting its participation in one or more fundamental cellular processes.

Based upon findings obtained in both cultured mammalian cells and a limited number of *BRCA1*^{-/-} breast and ovarian cancers, we proposed the existence of a significant relationship between the operations of p220 and the maintenance of elements of the heterochromatic su-

perstructure of the inactive X chromosome (Xi) (Ganesan et al., 2002). In particular, our results suggested a role for *BRCA1* in maintaining the concentration of the large noncoding RNA XIST on Xi. The evidence published in Ganesan et al. (2002) included low-level but significant overlap of *BRCA1* immunostaining with that of macrohistone H2A as well as with FISH staining of XIST RNA on Xi, the absence of XIST decoration of an X chromosome in a *BRCA1* mutant human tumor cell line and its reappearance after restoring wild-type (WT) p220 protein synthesis, marked reduction of XIST/Xi decoration following RNAi-mediated p220 depletion, and the absence of an inactive X chromosome in all members of a small collection of *BRCA1* mutant tumors. The mechanism linking XIST/Xi decoration to *BRCA1* function was not investigated beyond the finding that induction of *BRCA1* synthesis in a *BRCA1* mutant tumor cell line was accompanied by the appearance of XIST/Xi decoration but no increase in XIST abundance. By default, this suggested that *BRCA1* contributes to steps that support the concentration of XIST on Xi rather than playing a prime role in its synthesis or degradation. That notwithstanding, we indicated that one could not rule out from our results a more general role for *BRCA1* in regulating XIST synthesis.

Xiao et al. (2007), in this issue, question the validity of these conclusions, and we have taken their concerns to heart. As a first step, we have successfully reproduced the findings of Ganesan et al. (2002). Second, a new body of work has been completed, and the results of these studies are presented here. The new data reinforce and extend our original conclusions, which are also bolstered by the publication of complementary findings by others (Chadwick and Lane, 2005; Diaz-Perez et al., 2006; Ouyang et al., 2005). Specifically, we have confirmed the conclusion of Ganesan et al. that RNAi of *BRCA1* decreases XIST concentration on Xi by extending the RNAi results

from human to mouse cells using different target sequences. In addition, we have confirmed the relationship of BRCA1 to XIST concentration on Xi by demonstrating that depleting BRCA1 by Cre-mediated excision also decreases XIST concentration on Xi. Lastly, we demonstrate that mouse tumor lines derived from true *Brca1* null mammary tumors do not show XIST RNA concentration on Xi despite the presence of two X chromosomes.

RESULTS

A major claim of [Xiao et al. \(2007\)](#) (this issue of *Cell*) relates to whether BRCA1 colocalizes with XIST on Xi. Xiao et al. state that they lack consistent evidence to support our finding that a small minority of asynchronous cultured cells reveal colocalization of BRCA1 immunostaining and XIST FISH signals on the inactive X chromosome (Xi) ([Ganesan et al., 2002](#)). Second, Xiao et al. also question whether RNAi-mediated BRCA1 depletion affects XIST. They report that our data linking BRCA1 knockdown to decreased XIST signal on Xi are not reproducible. Finally, they question whether Xi is absent in *Brca1* mutant breast cancers. Contrary to [Ganesan et al. \(2002\)](#), Xiao et al. report that loss of BRCA1 function is not accompanied by concomitant loss of XIST/Xi decoration in *Brca1*^{-/-} murine tumors. We will address each of these points below.

Detection of BRCA1 at Xi

In their analysis, [Xiao et al. \(2007\)](#) have interpreted meaningful colocalization of BRCA1 and XIST to occur only when BRCA1 completely coats the territory of Xi with perfect coincidence of both images. This is a narrower definition of colocalization than we used. To be scored positive for colocalization, we required, at a minimum, a significant degree of apposition (i.e., partial fluorescent signal overlap) between BRCA1 and XIST or macrohistone H2A (mH2A), and this was repeatedly observed in a small minority of asynchronous cells in multiple cell lines.

Our work has been reproduced in part and extended by [Chadwick and Lane \(2005\)](#), who demonstrated significant costaining by both BRCA1 antibody and either mH2A or BUdR antibody of Xi in multiple human cell strains in late S phase. Multiple BRCA1 antibodies were used. These findings fit with our observation that “costaining was largely apparent in mid/late S phase cells.” Very recently, significant S phase-associated apposition of BRCA1 and Xi was also reported independently by others as part of a more general interaction of BRCA1 and replicating heterochromatin-dense chromosomal structures ([Pageau et al., 2006](#); [Pageau and Lawrence, 2006](#)).

Despite the call by [Xiao et al. \(2007\)](#) for a perfect fit of XIST and BRCA1 images as the only indicator of biological significance, it has been shown that certain Xi territory markers, such as H3K27 methylation, only partly overlap other Xi markers ([Chadwick and Willard, 2004](#); [Figure S3](#) in [Xiao et al., 2007](#)) because Xi heterochromatic territory is heterogeneous. Two distinct Xi regions, one marked by XIST, mH2A, and H3mK27 and the other by H3mK9

and HP1 γ (a BRCA1 partner protein; S.G. and D.M.L., unpublished data), have been detected ([Chadwick and Willard, 2004](#)). BRCA1 has been said to associate with both of these Xi territories, although likely at different times during Xi replication ([Chadwick and Lane, 2005](#)). Thus, perfect BRCA1/Xi marker costaining in asynchronous cells should be very uncommon or absent, as confirmed by Xiao et al., while partial overlap of XIST or other Xi-associated elements and BRCA1 in a minority of cells in an asynchronous culture would be an expected result. Notably, subsequent to our previous publication ([Ganesan et al., 2002](#)), other investigators published evidence of robust BRCA1/Xi costaining in mouse cells ([Diaz-Perez et al., 2006](#); [Ouyang et al., 2005](#)). We, too, continue to detect such an association in a minority of asynchronous cells (see [Figure S1](#) in the [Supplemental Data](#) available with this article online).

Given these findings, we would argue that our original evidence of BRCA1 immunostaining on a significant fraction of Xi territory in a small subset of unsynchronized cells has been reproduced and extended by newer results of other laboratories. The biochemical significance of these findings requires further work.

Effects of BRCA1 RNAi-Mediated Depletion on XIST Concentration on Xi

[Xiao et al. \(2007\)](#) report that attempts to knock down BRCA1 expression with RNAi failed to change the intensity of XIST/Xi signals. [Ganesan et al. \(2002\)](#) reported that RNAi-mediated depletion of BRCA1 in primary human cells led to suppression of XIST/Xi staining in many cells. Here we discuss the possible reasons for the difference in results with RNAi-mediated knockdown and present new data confirming our original RNAi data in another species.

With respect to the RNAi-mediated knockdown, we, too, have observed in some experiments using *BRCA1*-specific RNAi (even using the pooled, commercial *BRCA1* RNAi reagent that [Xiao et al. \[2007\]](#) used) that S phase BRCA1 nuclear dots largely disappear, but nothing happens to XIST. When BRCA1 protein levels were analyzed by western blots in these experiments, there was, typically, limited BRCA1 protein depletion (e.g., 50%–70%). However, when knockdowns approached $\geq 90\%$ or more, as seen in mouse X3 cells in [Figures 1A](#) and [1B](#), widespread reduction in XIST/Xi staining was observed. This may well be an indication that residual, low-level BRCA1 function is sufficient to support robust XIST/Xi staining. In this regard, BRCA1/BARD1 heterodimers are potent enzymes, and for a BRCA1 function (mitotic spindle development) for which its enzyme function is required, $>95\%$ BRCA1 protein depletion was needed to elicit an abnormal phenotype ([Joukov et al., 2006](#)). [Figures 1A](#) and [1B](#) support our earlier findings and weaken the case for off-target/nonspecific RNAi effects since this RNAi reagent targets a different sequence in a different species from those targeted in our prior results ([Ganesan et al., 2002](#)). There is also a technical matter worth considering. [Ganesan et al.](#) and the experiment depicted in [Figures 1A](#) and [1B](#) utilized an XIST RNA-FISH probe containing digoxigenin-modified nucleotides,

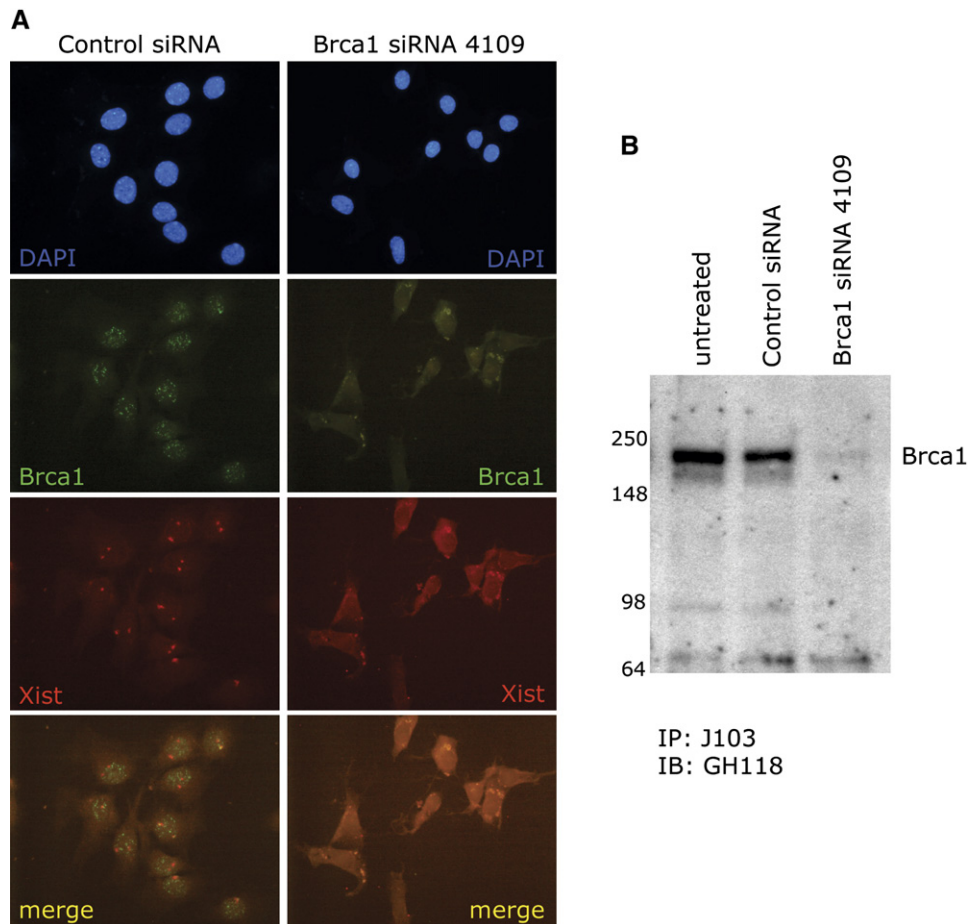


Figure 1. Effects of *Brca1* RNAi Treatment on XIST in Mouse X3 Cells

X3 cells were transfected with a *Brca1*-specific siRNA (number 4109, directed against a sequence in exon 12 of murine *Brca1*, an exon common to all known splicing variants of *Brca1*) or control siRNA. After a 24 hr incubation at 37°C, cells were split 1:3, and 48 hr later, they were fixed and subjected to BRCA1 immunostaining with a mouse monoclonal antibody to murine BRCA1 p220 followed by XIST RNA-FISH.

(A) BRCA1 and XIST RNA-FISH images of control- and 4109-transfected cells.

(B) In a separate experiment, an IP/western blot for BRCA1 was performed on X3 cells either mock transfected or transfected with luciferase-specific (control) or *Brca1*-specific siRNA. J103 is an affinity-purified rabbit antibody raised against a murine BRCA1 peptide sequence present in exon 8. GH118 is a murine monoclonal antibody directed against BRCA1.

visualized with a fluorescently labeled anti-digoxigenin antibody. We have subsequently observed that probes made with nucleotides directly coupled to fluorescent moieties visualize lower levels of XIST than digoxigenin-labeled ones. These types of probes were employed in the conditional mouse embryonic fibroblast (MEF) experiments below and by Xiao et al. Although the use of these more powerful probes tends to decrease the percentage of cells with no visible XIST in RNAi experiments compared with digoxigenin probes, clear reductions in XIST intensity are still present. Specifically, these more sensitive probes did not mask the overall finding that highly efficient RNAi of BRCA1 decreases the concentration of XIST on Xi in our hands.

Studies of *Brca1* and *Brca2* Conditional MEFs

As an independent and more stringent test of the hypothesis that loss of BRCA1 affects XIST/Xi decoration,

BRCA1 depletion was achieved and the state of XIST assessed in conditional *Brca1* knockout cells. Specifically, MEFs in which either one or two *Brca1* or *Brca2* conditional (floxed) alleles were present were analyzed. In the conditional *Brca1* allele, exons 5–13 are flanked by loxP sites, and in the conditional *Brca2* allele, exon 11 is flanked by loxP sites (Clark-Knowles et al., 2007; Jonkers et al., 2001). When exposed to Cre, these conditional *Brca1* and *Brca2* alleles develop into null alleles. When *Brca1*^{fllox/fllox} MEFs were exposed to a self-excising, Cre-encoding retrovirus (Silver and Livingston, 2001), levels of BRCA1 p220 fell dramatically, without an effect on the BRCA2 protein (Figure 2A). The opposite was true in infected *Brca2*^{fllox/fllox} MEFs. Furthermore, in independent experiments, Cre transduction resulted in efficient genomic deletion as judged by Southern blotting (Figure 2B) and elimination of BRCA1 protein immunostaining in S phase cells

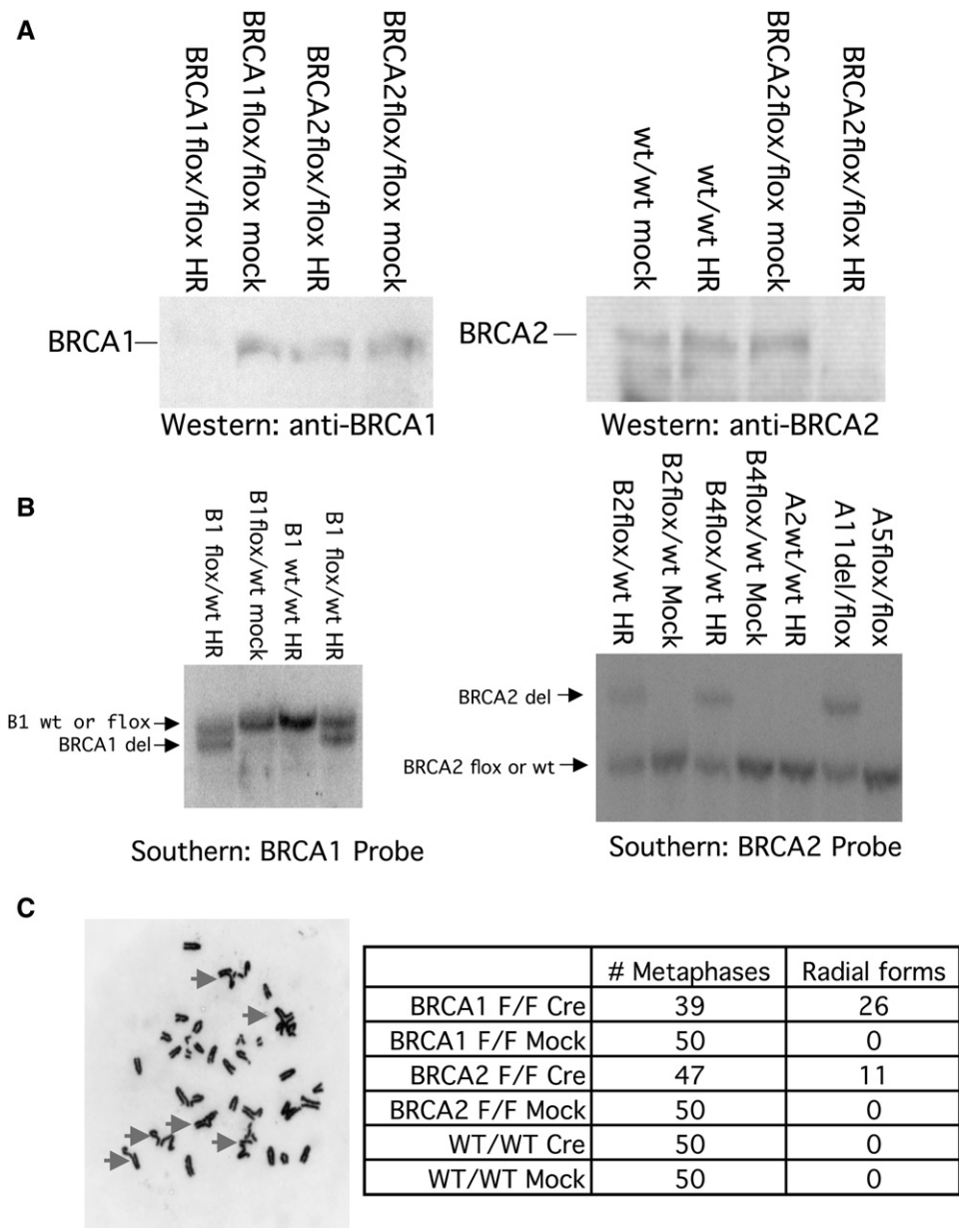


Figure 2. Cre Infection Leads to Efficient Excision of Conditional *Brca1* and *Brca2* Alleles, Loss of Protein Expression, and Induction of Genomic Instability

MEFs carrying conditional (floxed) or WT alleles of *Brca1* or *Brca2* were either infected or mock infected with a self-deleting Cre retrovirus (HR = hit-and-run self-excising Cre retrovirus; Silver and Livingston, 2001).

(A) Western blots of protein extracts from either mock-infected or Cre-infected *Brca1*^{flox/flox} and *Brca1*^{WT/WT} MEFs using a BRCA1-specific antibody are shown in the left panel. Western blots of protein extracts from mock- or Cre-infected *Brca2*^{flox/flox} and *Brca2*^{WT/WT} MEFs using a BRCA2-specific antibody are shown in the right panel.

(B) Southern blots were performed on DNA extracted from Cre- or mock-treated MEFs containing *Brca1*^{flox/WT} alleles (left panel) or *Brca2*^{flox/WT} alleles (right panel) and probed with *Brca1*- or *Brca2*-specific DNAs, respectively. Expected sizes of the WT, floxed, and del alleles are shown. In both cases, two separate MEF strains of floxed/WT genotype are shown. In the right panel, additional controls of Cre-treated *Brca2*^{del/flox} (A11) and *Brca2*^{flox/flox} MEFs (A5) are shown.

(C) Deletion of the *Brca1* gene by Cre-mediated excision results in the development of chromosomal instability. *Brca1* conditional MEFs of the genotype *Brca1*^{flox/flox} were either infected or mock infected with a self-deleting Cre retrovirus. Seventy-two hours later, chromosomal spreads were prepared. An example of a chromosomal spread from the Cre-treated *Brca1*^{flox/flox} MEFs is shown in the left panel, with quadriradial chromosomes or fragments of quadriradial forms indicated by arrows. The number of metaphase spreads examined and number of radial forms found are shown in the table to the right. All chromosomal spreads were analyzed with the observer blinded to the history and identity of the cells.

(Figure S3A). The presence of a *Rosa26* locus-embedded lox-stop-lox-*lacZ* allele (*R26R*) (Soriano, 1999) in some of these MEF strains permitted assessment of Cre activity. Efficient Cre-mediated deletion was reflected by lacZ-dependent X-gal staining in >90% of cells in the Cre-infected MEFs containing the *R26R* allele (data not shown).

A different manifestation of the absence of BRCA1 or BRCA2 function was also observed in Cre-treated conditional cells (Figure 2C and Figure S3B). In both Cre-treated *Brca1*^{flox/flox} and *Brca2*^{flox/flox} MEFs, significant numbers of cells revealed quadriradial chromosome formation (likely a manifestation of illegitimate recombination) within 72 hr after infection. No such structures were observed in Cre-infected WT MEFs, showing that Cre alone did not elicit them, nor were they seen in naive, untreated cells of any genotype. Furthermore, quadriradial chromosomes were absent after Cre infection of MEFs bearing conditional *R26R* alleles but no *Brca1* or *Brca2* conditional alleles (data not shown). Thus, their appearance was a sign of BRCA1 or BRCA2 depletion rather than merely of Cre activity. Therefore, MEFs rendered *Brca1*^{-/-} by Cre infection revealed independent evidence of a loss of a fundamental BRCA1 function, genome integrity maintenance.

Five days after Cre virus or mock infection, XIST RNA-FISH was performed on conditional *Brca1*, conditional *Brca2*, and control MEFs, and an investigator blinded to the identity of the cultures being analyzed obtained multiple photomicrographs from each. The photomicrographs were scored for XIST/Xi staining intensity by four blinded analysts (Figure 3 and Figure S2). Representative pictorial examples of such fields and a semiquantitative analysis of the results obtained by the blinded analysts revealed that only cells that had lost both *Brca1* alleles experienced an overt, statistically significant ($p < 0.0001$) reduction in focal XIST/Xi staining by comparison with controls analyzed in parallel (Figure 3C). Similar results were obtained using MEFs of the same genotypes derived from separate embryos in an independent experiment (data not shown). The reduction in XIST/Xi intensity in *Brca1* null cells was not a result of a proliferation block/defect, because no such reduction was observed in *Brca2* null cells, which experienced a proliferation effect similar to *Brca1* null cells (Patel et al., 1998; Xu et al., 1999). Indeed, FACS analyses of *Brca1*^{-/-} and *Brca2*^{-/-} MEFs generated by this approach revealed no major changes in the distribution of cell-cycle intervals from that of Cre-treated WT MEFs. This implies that the proliferation defect in the nullizygous cells was a result of a general slow-down in cell-cycle progression (D.P.S. and D.M.L., unpublished data).

Hence, acute homozygous *Brca1*, but not *Brca2*, loss of function in conditional MEFs resulted in a significant diminution in the intensity of XIST/Xi staining.

XIST/Xi in Breast Tumors Arising in *Brca1* Germline Mutant Mice

Xiao et al. (2007) report that cells of mammary tumors arising in mice engineered to produce a homozygous *Brca1* mutation ($\Delta 11/\Delta 11$) in mammary tissue contain XIST/Xi

foci. The authors argue that this result runs counter to our observations that human *BRCA1*^{-/-} tumors lack robust XIST and H3meK27/Xi foci (Ganesan et al., 2002). Here we discuss possible reasons for the discrepancies in the results and report new data examining XIST staining and localization in cell lines derived from *Brca1* null tumors generated in a conditional *Brca1* knockout mouse model.

In our view, the discrepancy between our original results and those of Xiao et al. (2007) may reflect the nature of the different *Brca1* mutations in the two sets of experiments. *Brca1* $\Delta 11$, the mouse *Brca1* mutant allele studied by Xiao et al., is a hypomorph, not a null mutation (Brodie and Deng, 2001). It results from a clean deletion of *Brca1* exon 11 and, unlike null mutants, leaves intact a normal, naturally occurring alternatively spliced BRCA1 protein, $\Delta 11$. *Brca1*^{-/-} (null) mutant murine embryos die early in embryogenesis, even when bred onto a *p53* mutant background (Ludwig et al., 1997). In contrast, *Brca1* ^{$\Delta 11/\Delta 11$} ; *p53*^{+/-} mice are born and become viable adults (Xu et al., 1999, 2001). The females tend to develop mammary tumors. Moreover, the $\Delta 11$ protein retains certain WT p220-like properties both in mitotic cells (Huber et al., 2001) and in a minority of pachytene spermatocytes (Turner et al., 2004). In addition, some organisms completely lack an exon 11-like unit; for example, the WT *C. elegans* *BRCA1* ortholog lacks these sequences yet performs normal DNA damage-response functions (Boulton et al., 2004). Finally, BRCA1 $\Delta 11$ protein retains an ability to localize in subnuclear foci indistinguishable from BRCA1 p220 (Huber et al., 2001). Since $\Delta 11$ retains certain WT BRCA1 functions, it is difficult with the available evidence to know whether $\Delta 11$ mammary tumors emerge via the same molecular and biological pathway (or pathways) as null *BRCA1*^{-/-} human tumors. In addition, mammary epithelial cell-associated *p53* mutations alone can give rise to murine breast cancer (Lin et al., 2004), raising the question of whether some of the $\Delta 11$ tumor cells analyzed in Xiao et al. are actually *Brca1* WT, *p53* mutant. We have found that cell lines derived from tumors arising in *Brca1* conditional, *p53* conditional mammary epithelia exposed to Cre are not infrequently *p53* mutant but *Brca1* WT. Xiao et al. offer no evidence that the tumor lines that they analyzed harbor *Brca1* mutations. In fact, at least one of the cell lines analyzed in Xiao et al., W0069, appears to be *Brca1* WT (Figure S4). Hence, for the reasons noted here, the presence of a normal Xi in cells derived from murine $\Delta 11$ mammary tumors analyzed in Xiao et al. might not be remarkable. In this regard, the human L56Br-C1 cell line studied by Xiao et al. and found to contain XIST/Xi structures carries a translation-terminating *BRCA1* mutation within exon 11 that should, in principle, leave the endogenous $\Delta 11$ mRNA intact (Johannsson et al., 2003). If $\Delta 11$ protein positively influences XIST/Xi costaining, this line could have retained that function.

To determine the status of XIST localization in murine tumors carrying true null *Brca1* alleles, we have employed a conditional *Brca1* mouse model in which exons 5–13 are flanked by loxP sites (the same allele used in the *Brca1*

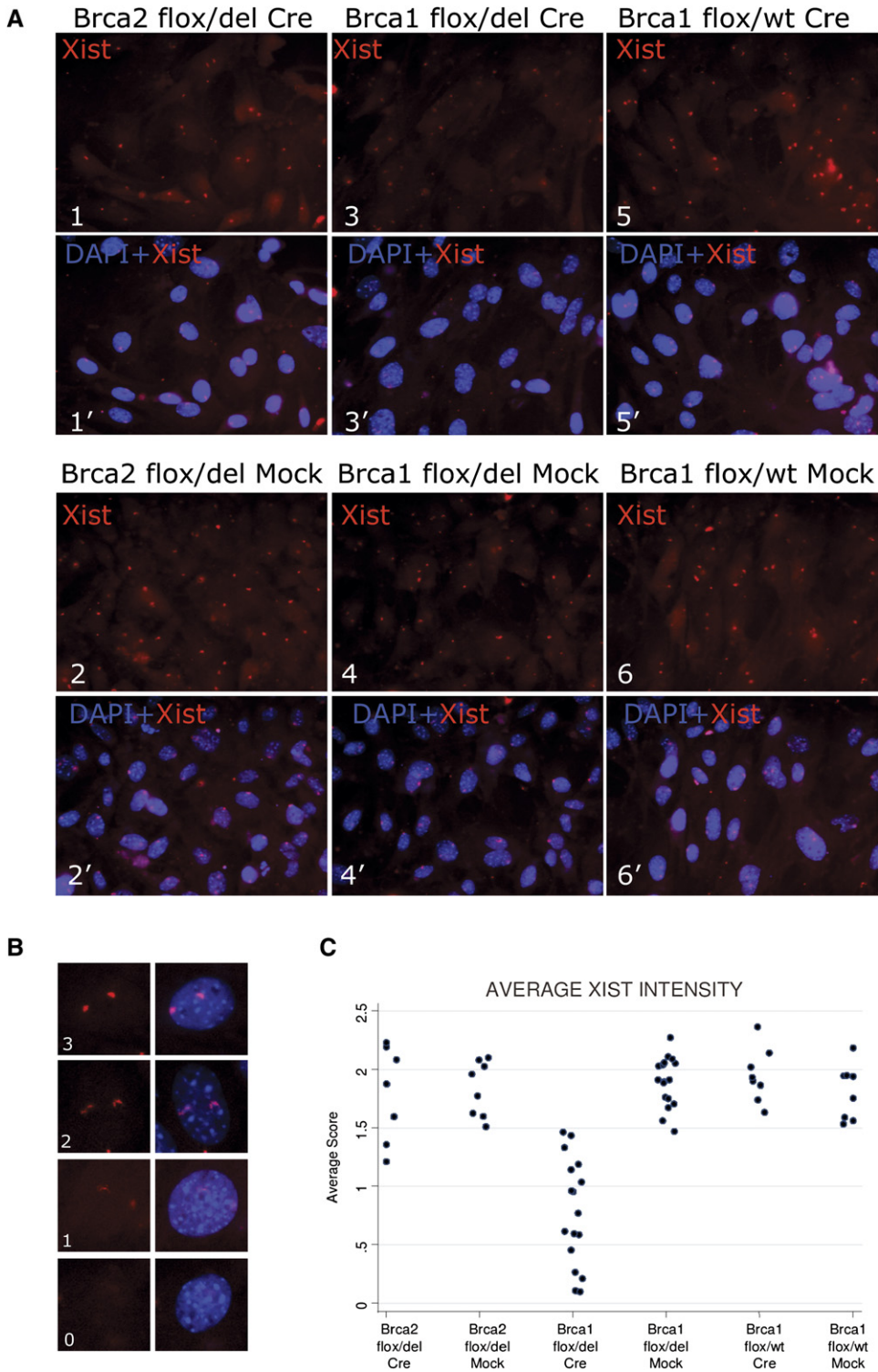


Figure 3. Effect of Cre-Mediated *Brca1* Excision on XIST/Xi Staining

MEFs were prepared from embryos containing alleles with loxP sites encompassing exons 5–13 of *Brca1*, labeled *Brca1*^{flox} (Clark-Knowles et al., 2007); alleles with loxP sites encompassing exon 11 of *Brca2* (Jonkers et al., 2001), labeled *Brca2*^{flox}; corresponding *Brca1*^{del} or *Brca2*^{del} alleles; or WT *Brca1* alleles, as indicated. Early-passage MEFs were infected with a self-excising Cre retrovirus on two successive days or were handled identically except that virus was not added. Cells were split once after infection, and RNA-FISH for XIST was performed 5 days after the first infection using a probe derived from murine *Xist* using nick translation incorporating Spectrum Red dUTP per the manufacturer's instructions.

floxed MEFs described above). The Jonkers laboratory has used these mice to generate *Brca1* null mammary carcinomas using a cytokeratin 14 promoter-driven Cre transgene (*K14cre*; Jonkers et al., 2001) in the context of conditional *p53*. In a blind analysis performed in three separate laboratories, none of the cultures of six independently derived clonal cell lines from two *Brca1* null tumors revealed focal XIST spots (Figure 4A). The absence of XIST spots was not a result of X monosomy, given the presence of at least two X chromosomes in cells of these tumor lines when analyzed by DNA-FISH (Figure 4B). The *Brca1* null genotype of each line was confirmed by allele-specific PCR, and all six lines lacked BRCA1 nuclear foci when examined by immunofluorescence (data not shown). Cells derived from control mammary tumors in which only *p53* was targeted showed both intact BRCA1 nuclear foci and robust focal XIST staining (Figure 4 and data not shown).

To explore the XIST status of additional *BRCA1* mutant cell lines, we have recently performed XIST RNA-FISH on the five human *BRCA1* mutant cell lines available in our laboratory, four of which were not known to be *BRCA1*^{-/-} in 2002—i.e., HCC1395, SUM149PT, SUM1315MO2 (Elstrodt et al., 2006), and L56Br-C1. HCC1937, long known to be *BRCA1*^{-/-}, was also tested. Only L56Br-C1 displayed focal XIST staining, whereas focal XIST could not be detected in the other four lines (Figure S5). We agree with Xiao et al. (2007) that there are undoubtedly *BRCA1* WT cell lines and tumors that lack focal XIST staining, most likely a result of Xi loss. However, among *BRCA1*^{-/-} carcinomas, loss of focal XIST staining was more common than in breast carcinomas—even high grade lesions—of other pathological subtypes (Richardson et al., 2006).

The human tumor data in our original paper have been confirmed in a more recent analysis from our group (Richardson et al., 2006). We report a lack of focal XIST and H3meK27 spots in all five new human *BRCA1*^{-/-} breast carcinoma samples examined. This paper also described a similar XIST/Xi loss phenotype in 14 out of 17 cases of sporadic basal-like breast cancer. Sporadic basal-like carcinomas are *BRCA1* WT yet are a known *BRCA1*^{-/-} breast carcinoma phenocopy, sharing a similar gene expression pattern, a similar estrogen and progesterone receptor and cytokeratin expression phenotype, a lack of *HER2* amplification, and *p53* mutation status with *BRCA1*^{-/-} breast cancers (Richardson et al., 2006; Sorlie et al., 2003). Thus, it is tempting to speculate that the sporadic basal-like breast cancers are defective in a pathway (or pathways) in which BRCA1 participates

and may, therefore, share XIST loss with hereditary *BRCA1*^{-/-} breast cancers. This notwithstanding, given the relatively small number of tumors analyzed, there may well be some *BRCA1*^{-/-} human tumors with XIST/Xi structures. The nature of the relevant *BRCA1* mutant genotypes in settings where XIST is absent compared to any where it is present would need to be considered. If, as suggested by Xiao et al. (2007), low-level XIST synthesis from Xa occurs, this, too, could account for XIST foci in some tumor cells.

DISCUSSION

We believe that the data reported here help to explain the apparent discrepancies noted by Xiao et al. (2007) and reinforce the view that BRCA1 influences, directly or indirectly, XIST decoration of Xi in adult somatic cells. Xiao et al. present four lines of evidence in support of their view that BRCA1 does not influence XIST localization. First, they argue that BRCA1 does not “coat” the inactive X chromosome. However, in Ganesan et al. (2002), no claim was made that BRCA1 perfectly coats Xi or provides the prime force that drives XIST/Xi coating, e.g., during embryogenesis; rather, in a small percentage of cells, a percentage that varied among the cell types examined, BRCA1 exhibited overlapping staining with XIST or with a marker of Xi, macrohistone H2A. Though quantitation likely varies among observers and cell lines and as a function of the scoring criteria used, a small minority of cycling cells showed significant overlap of BRCA1 and markers of Xi in Xiao et al. and Ganesan et al. Furthermore, an association of BRCA1 with markers of Xi has now been published by at least three independent laboratories (Chadwick and Lane, 2005; Diaz-Perez et al., 2006; Pageau et al., 2006).

Second, Xiao et al. (2007) show an analysis of XIST in HCC1937, a *BRCA1*^{-/-} tumor line, and the effect of BRCA1 reconstitution of that line. Much of the apparent disagreement between Ganesan et al. and Xiao et al. regarding these experiments is likely explained by the chromosomal instability of this line. The subclone used in Ganesan et al. was itself a mixture of cells containing two X chromosomes and a minor population with many more X chromosomes. Subsequent work with HCC1937 has shown that the chromosomal content of this line has evolved quickly with passage, and different cultures of this line differ considerably in chromosomal content (A. De Nicolo and D.M.L., unpublished data). We strongly

(A1–2') XIST RNA-FISH analysis of *Brca2*^{flox/del} MEFs treated with Cre-encoding retrovirus (upper panels) or mock infected (lower panels). (A3–4') XIST RNA-FISH staining of *Brca1*^{flox/del} MEFs treated with Cre-encoding retrovirus (upper panels) or mock infected (lower panels). (A5–6') XIST RNA-FISH staining of *Brca1*^{flox/WT} MEFs treated with Cre-encoding retrovirus (upper panels) or mock infected (lower panels). The exposure time for each XIST micrograph was the same throughout. Similarly, the exposure time for the DAPI micrographs was held constant. (B) Four assigned intensity categories (0, 1, 2, and 3) used as a training slide for scoring XIST intensity. (C) Semiquantitative analysis of the intensity of XIST signals in *Brca2*^{flox/del}, *Brca1*^{flox/del}, and *Brca1*^{flox/WT} MEFs 5 days after infection with Cre or mock treatment. Photomicrographs of multiple fields from each cell strain were blindly analyzed by four independent analysts, who categorized each nucleus for XIST signal strength according to the standards in (B). The XIST intensity was averaged over the cells in each field for each analyst (see Experimental Procedures), and each such average is represented as a single point on the graph. An exact two-sided Wilcoxon rank-sum test revealed a significant difference ($p < 0.0001$) between XIST intensity in *Brca1*^{flox/del} Cre-infected cells compared to the other five groups combined.

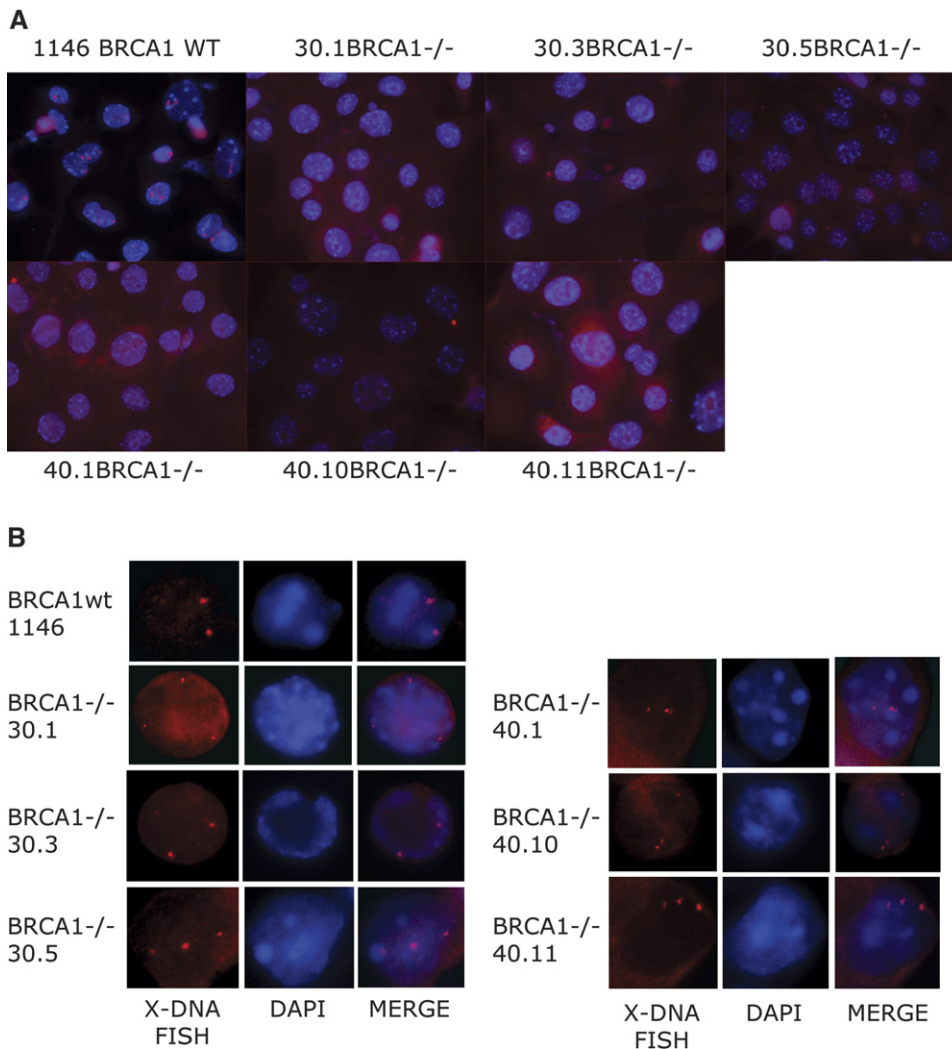


Figure 4. Cell Lines Derived from *Brca1*^{-/-};*p53*^{-/-} Murine Breast Cancers Lack XIST Foci

Cell lines were obtained from tumors that arose in mice homozygous for a conditional *Brca1* allele in which exons 5–13 of *Brca1* were flanked by loxP sites, homozygous for a conditional *p53* allele, and carrying a cytokeratin 14 promoter-driven Cre allele. These breast cancers and derived cell lines had a *Brca1*^{-/-};*p53*^{-/-} genotype as shown by direct genotyping. A control cell line (1146) was obtained from a breast cancer that arose in a mouse with WT *Brca1* but conditional *p53* and cytokeratin 14-driven Cre. Its genotype was *Brca1*^{+/+};*p53*^{-/-}.

(A) All cell lines were subject to RNA-FISH for XIST RNA. The RNA-FISH signal is shown in red, and the DAPI nuclear signal is shown in blue for all cell lines tested.

(B) X chromosome DNA-FISH analysis of murine *Brca1*^{-/-} cell lines. *Brca1* WT (1146) and six *Brca1*^{-/-} mouse mammary tumor cell lines (30.1, 30.3, 30.5, 40.1, 40.10, and 40.11) were grown on coverslips and processed for DNA-FISH using a probe specific for the murine X chromosome. For each cell line, the DNA-FISH signal is shown in red (left panel) and DAPI nuclear staining in blue (middle panel), and a merged image is shown in the right panel.

suspect that the inability of Xiao et al. to restore strong, focal XIST staining may relate to differences in the X chromosomal content of subclones. Early passages of BRCA1-reconstituted HCC1937 were sent to another laboratory, and they reproduced our finding that, unlike either parental HCC1937 or vector-reconstituted HCC1937, the majority of BRCA1-reconstituted HCC1937 showed focal XIST staining, with the majority of these cells having two X chromosomes (Pageau et al., 2006). While another BRCA1-reconstituted HCC1937 subclone showed no

focal XIST, it contained only one X chromosome (Pageau et al., 2006).

Third, the RNAi experiments of Xiao et al. (2007) were interpreted by the authors to reveal no effect of BRCA1 RNAi on XIST staining. However, close examination of their figures suggests a dimming of XIST intensity in the presence of BRCA1 RNAi in their Figure 3H compared with their Figure 3G and in their Figure S5B compared with their Figure S5A, in general agreement with observations made by Ganesan et al. (2002). Perhaps some of these differences

in interpretation are based on the view that XIST coating of Xi is an “all or nothing” phenomenon. Our experiments and others that we are aware of suggest that XIST is in dynamic equilibrium with Xi and that the initiation and maintenance of XIST coating may be separable functions. Whatever the case, the conditional knockout of BRCA1 avoids the pitfalls of incomplete RNAi and demonstrates an effect of BRCA1 loss on XIST/Xi intensity.

Xiao et al. (2007) analyzed murine tumors and cell lines derived from them that were all generated in a mouse model that deletes *Brca1* exon 11. As described above, this is a hypomorphic mutation (Brodie and Deng, 2001). Because this mutation preserves a naturally occurring BRCA1 isoform, $\Delta 11$, it is difficult to predict what the outcome of such a knockout would be on any particular BRCA1 function. Furthermore, as discussed above, the *Brca1* ^{$\Delta 11/\Delta 11$} genotypic status of the tumors presented in Xiao et al. is unclear since at least one of them examined by us appears to be *Brca1* WT (Figure S4). Xiao et al. also presented an analysis of RNA expression of genes along the X chromosome in both embryonic and mammary tissue from $\Delta 11$ homozygous mice compared with $\Delta 11$ heterozygous mice to show that BRCA1 loss does not influence Xi silencing. However, Ganesan et al. (2002) did not claim a global failure of Xi silencing or widespread reactivation of X-linked genes as a result of BRCA1 loss. What was observed was a low-level reactivation of a GFP reporter embedded in Xi following BRCA1 depletion and, in later work, upregulation of a small subset of X-encoded genes in five *BRCA1*^{-/-} breast carcinomas (Richardson et al., 2006).

Xiao et al. have also argued that our results demonstrating Xi loss in sporadic basal-like cancer (BLC), a *BRCA1* WT tumor, invalidate the argument that Xi loss in *BRCA1*^{-/-} tumors is a *BRCA1* mutation-associated event. However, as discussed above, sporadic BLCs are well-known phenocopies of *BRCA1*-deficient tumors (Turner et al., 2004; Lacroix and Leclercq, 2005). Not unexpectedly, then, sporadic and *BRCA1* mutant BLCs share another property—i.e., loss of a normal Xi, a feature that is rare in aggressive, nonbasaloid breast cancer cases (Richardson et al., 2006).

Moreover, the tumor cells of a majority of the *BRCA1*^{-/-} and sporadic basal-like tumors that have been reported have undergone X isodisomy, with the active X being duplicated and Xi lost (Richardson et al., 2006). On its face, this would seem to be at odds with the notion that BRCA1 abundance contributes to active XIST/Xi decoration. However, it is worth noting that BRCA1 is a multifunctional protein, one operation of which is to promote stable mitotic spindle pole and spindle formation (Joukov et al., 2006). Another is to participate in centrosome operations (Parvin and Sankaran, 2006; Xu et al., 1999). In the absence of sufficient BRCA1 p220, spindle formation is compromised, resulting in a variety of abnormal mitotic phenotypes. Moreover, aneuploidy is known to develop shortly after loss-of-function mutation of both copies of the *BRCA1* gene (Shen et al., 1998), and the genomes of

BRCA1^{-/-} and sporadic basal-like tumors are overtly unstable (Chappuis et al., 2000). This may help to explain why chromosomal abnormalities (including X isodisomy) are so prevalent in cells that have either lost BRCA1 function *per se* or encountered defects in pathways in which BRCA1 normally participates.

There being no *a priori* or independent evidence that BRCA1 operates as a dosage-compensation element, we speculate that it plays a different kind of role in the biology of Xi. BRCA1 is a genome integrity maintenance protein that contributes to DNA repair, checkpoint activation, mitotic spindle development, and possibly the centrosome cell cycle (Gudmundsdottir and Ashworth, 2006; Joukov et al., 2006; Parvin and Sankaran, 2006). Thus, communication between BRCA1 and XIST/Xi might be a manifestation of a BRCA1 genome integrity maintenance function. In this regard, recent evidence from Marahrens and coworkers (Diaz-Perez et al., 2006) strongly suggests that engineered loss of the *Xist* gene is associated with subsequent X chromosomal damage. Moreover, a replicating Xi is reported to accumulate γ -H2AX (Chadwick and Lane, 2005), a signal that often reflects DNA damage—e.g., double-strand breaks associated with stalled replication forks. In this context, one wonders whether failure of XIST to concentrate on Xi in the absence of BRCA1 promotes damage to and subsequent loss of Xi and, if so, whether loss of Xi in that setting is compensated by the duplication of Xa. Finally, Pageau and Lawrence (2006) have shown that BRCA1 displays a significant association, especially during S phase, with certain heterochromatin-containing nuclear structures, Xi being but one of them. This set of findings raises the interesting possibility that communication between BRCA1 and Xi may well be a reflection of a larger role for BRCA1 in maintaining heterochromatin structure or function.

EXPERIMENTAL PROCEDURES

Brca1 RNAi in Mouse Cells

$2 \times 10^4/\text{cm}^2$ cells were plated on glass coverslips in six-well plates and incubated overnight at 37°C in DMEM + 10% FBS + Pen/Strep. After 24 hr, cells were transfected with either a control siRNA or a *Brca1*-specific siRNA 4109 (directed against a sequence in exon 12 of murine *Brca1*; 5'-TCCGGATACGAGAGTGAAA-3') using Lipofectamine 2000 transfection reagent (Invitrogen) following the manufacturer's protocol. Ten microliters of each 20 μM siRNA (Dharmacon) was diluted in 250 μl of Opti-MEM I medium (Invitrogen). Ten microliters of Lipofectamine 2000 was diluted in 250 μl of Opti-MEM I, incubated for 5 min at room temperature, and added to the diluted siRNA. After 20 min of incubation at room temperature, samples were added to the individual wells containing 2 ml DMEM + 10% FBS. After 24 hr of incubation at 37°C, cells were split 1:3, plated on glass coverslips in six-well plates, and analyzed 48 hr later.

Conditional Deletion of *Brca1* and *Brca2*

MEFs were prepared from embryos containing alleles with loxP sites encompassing exons 5–13 of *Brca1*, labeled *Brca1*^{fllox} (Clark-Knowles et al., 2007); embryos containing with loxP sites encompassing exon 11 of *Brca2* (Jonkers et al., 2001), labeled *Brca2*^{fllox}; embryos with corresponding germline deletions; or embryos containing WT *Brca1* or *Brca2* alleles. Early-passage MEFs were infected with a self-excising

Cre retrovirus (Silver and Livingston, 2001) on two successive days or were handled identically, except that virus was not added. For XIST experiments, cells were split once after infection, and RNA-FISH for XIST was performed 5 days after the first infection.

Derivation of Mouse Tumor Lines

To generate *Brca1*^{-/-}; *p53*^{-/-} and *Brca1*^{WT/WT}; *p53*^{-/-} murine breast cancer cell lines, two individual spontaneous mammary tumors (numbers 30 and 40) that developed in *K14cre*; *Brca1*^{lox/flox}; *p53*^{lox/flox} mice and one that developed in a *K14cre*; *Brca1*^{WT/WT}; *p53*^{lox/flox} mouse (X.L. et al., unpublished data) were collected aseptically by blunt dissection. Tumors were mechanically dissociated by mincing and sorted through a 40 μ m Falcon strainer to remove larger tumor cell aggregates. Cells were cultured in DMEM/F12-GlutaMAX (GIBCO) supplemented with 10% fetal bovine serum (Greiner Bio-One), 5 μ g/ml insulin (Sigma), 5 ng/ml EGF (Invitrogen), and 5 ng/ml cholera toxin (Sigma) and incubated at 37°C under 5% CO₂. Four days later, fibroblasts were removed by partial digestion with 1 \times trypsin-EDTA (GIBCO), and epithelial subpopulations were selected manually. Once regrown, clonal cell lines were derived from these subpopulations by limiting dilution, and the clones were genotyped as described (X.L. et al., unpublished data).

Indirect Immunofluorescence

Mouse cells grown on glass coverslips were washed three times with PBS, fixed in 3% paraformaldehyde/2% sucrose solution for 10 min at room temperature, washed twice with PBS, and permeabilized with PBS/0.05% Triton X-100 for 5 min at room temperature. Cells were then incubated with primary anti-BRCA1 monoclonal antibody GH118 in 4 \times SSC, 1 μ g/ μ l BSA, 0.5 μ g/ μ l salmon sperm DNA, 10 U/ μ l RNasin for 1 hr at 37°C; washed twice for 5 min in PBS; and incubated with a FITC-conjugated goat anti-mouse secondary antibody (Jackson ImmunoResearch) for 1 hr at 37°C, followed by three PBS washes. Coverslips were processed further for RNA-FISH or mounted on slides with DAPI-containing mounting medium (Vector Laboratories) and kept at 4°C until analysis. For immuno-RNA-FISH, cells were fixed again as above with paraformaldehyde/sucrose and processed for RNA-FISH.

RNA-FISH

Cells were washed three times in PBS, fixed in 3% paraformaldehyde/2% sucrose solution for 10 min at room temperature, washed twice in PBS, permeabilized with PBS/0.05% Triton X-100 for 5 min at room temperature, washed again three times in PBS, incubated in cold 70% ethanol for 2 hr at 4°C, incubated for 10 min in ice-cold 100% ethanol, and air dried. For the mouse X3 cell experiments, *Xist* probe was prepared by labeling with digoxigenin-11-dUTP (DIG-Nick Translation Mix, Roche Applied Science). One microgram of plasmid encoding mouse XIST and 4 μ l DIG-Nick Translation Mix were resuspended in double-distilled water to a final volume of 20 μ l and incubated for 2.5 hr at 15°C. The reaction was stopped by addition of 2.5 μ l of 10% SDS and 5 μ l of 0.5 M EDTA (pH 8.0) followed by incubation for 10 min at 90°C. After precipitation with 0.1 vol 3 M NaOAc, 2.5 vol 100% EtOH, and 2 μ l salmon sperm DNA (10 mg/ml)/tRNA (10 mg/ml) (Invitrogen), probe was washed with 70% EtOH, air dried, and resuspended in 80 μ l double-distilled water. Five microliters of this digoxigenin-labeled *Xist* probe, 12 μ l of human Cot-1 DNA (Invitrogen), and 2 μ l salmon sperm DNA/tRNA were mixed and dried in a speed vacuum for 35 min. The pellet was resuspended in 10 μ l of 100% formamide and denatured for 10 min at 95°C. After addition of 10 μ l of 4:1 mix of RNA hybridization buffer (1 ml 7.5% BSA, 1 ml 20 \times SSC, 2 ml 50% dextran sulfate)/VRC (vanadyl ribonucleoside complex, Invitrogen), the mix was applied to the coverslip and hybridized overnight at 37°C. Coverslips were washed for 20 min in 50% formamide/2 \times SSC at 37°C, 20 min in 2 \times SSC at 37°C, and 20 min in 1 \times SSC at room temperature; incubated in anti-digoxigenin secondary antibody (1:200 in 4 \times SSC, 1% BSA) for 1 hr at 37°C; and washed in 4 \times SSC for 10 min at room temperature, 4 \times SSC/0.1% Triton X-100 for 10 min at room temperature, and 4 \times SSC for an additional 10 min at room

temp. Coverslips were mounted on slides with DAPI-containing mounting medium (Vector Laboratories) and kept at 4°C until analysis.

For the experiments with conditional MEFs, 1 μ g of a plasmid encoding mouse XIST was directly labeled per the manufacturer's instructions (Vysis). The probe was then ethanol precipitated, washed in 70% ethanol, and air dried. The probe was then resuspended in 225 μ l RNA hybridization buffer (1 part 20 mg/ml BSA, 1 part 20 \times SSC, 2 parts 50% dextran sulfate) to make a probe stock. Four parts of probe stock were diluted in 1 part VRC and 5 parts 100% formamide, denatured at 80°C for 10 min, and hybridized overnight at 37°C. The slides were then washed and processed as above.

DNA-FISH

Murine cell lines were grown on glass coverslips, fixed in 3% buffered paraformaldehyde, and processed for DNA-FISH as described previously (Clemson et al., 1996; Lee and Jaenisch, 1997). To prepare murine X chromosome-specific probes, murine X chromosome BACs (51A16 and 23H12) validated for FISH were used (Korenberg et al., 1999). Digoxigenin-labeled probes were generated from these BAC templates using a DIG-Nick Translation Kit (Roche Applied Sciences). After hybridization with labeled probe, cells were then incubated with rhodamine-labeled anti-digoxigenin Fab fragments at a final concentration of 1 μ g/ml (Roche Applied Sciences). After washing, coverslips were mounted on glass slides with Vectashield containing DAPI (Vector Labs). Staining was visualized on a Zeiss Axiophot fluorescence microscope, and images were captured with a CCD camera.

Southern and Western Blots

Southern blotting was performed with high-salt buffer as described (Ausubel et al., 1999). Hybond-XL membrane and Ambion ULTRAhyb were used per the manufacturer's instructions. A probe consisting of exon 14 sequences from murine *Brca1* was prepared by digesting the murine *Brca1* cDNA with BglII and SacI, isolating the resulting 257 bp fragment, and labeling with ³²P using a Boehringer Mannheim Random Primed DNA Labeling Kit. A probe for murine *Brca2* exon 14 was prepared by PCR using the forward primer 5'-GCTTCTGTCTAAAGGG CATC-3' and the reverse primer 5'-TCTTCCTGTCTCCATCT-3'. Total genomic DNA was digested with EcoRV in the case of *Brca1* and KpnI in the case of *Brca2*. Digested genomic DNA was electrophoresed on a 0.7% agarose gel.

For immunoblots, cell extracts were prepared in NETN (150 mM NaCl, 1 mM EDTA, 20 mM Tris [pH 8.0], 0.5% NP40). Semidry western transfers were performed as described in Scully et al. (1997). Signals were detected by ECL (Amersham). Murine BRCA1 was visualized with monoclonal antibody GH118 (Ganesan et al., 2002) and murine BRCA2 with a polyclonal affinity-purified anti-BRCA2 antibody (D.P.S. and D.M.L., unpublished data).

Chromosome Spreads

Brca1 conditional MEFs of the various genotypes were either infected or mock infected with a self-deleting Cre retrovirus. Seventy-two hours later, chromosomal spreads were prepared as described in Silver and Livingston (2001).

Statistical Methods

Photomicrographs were made for each of the six categories of MEFs in Figure 3. Experimenters blind to the genotype of the MEFs scored each as having XIST intensity 0, 1, 2, or 3 based on the training slides in Figure 3B. For each experimenter on each photomicrograph, the average XIST intensity score (over all cells in the photomicrograph) was calculated, and the averages from the *Brca1*^{lox/del} Cre were compared to the averages from the other types of MEF using a two-sided exact Wilcoxon rank-sum test.

Supplemental Data

Supplemental Data include five figures and can be found with this article online at <http://www.cell.com/cgi/content/full/128/5/991/DC1/>.

ACKNOWLEDGMENTS

We wish to extend our thanks to J. Lawrence and G. Pageau for helpful discussions and for sharing the results of their BRCA1/heterochromatin association experiments prior to publication. We would also like to acknowledge the contributions of S. Pathania and B. Liu (DFCI) for help with scoring photomicrographs; K. McKinney and M. Brown (DFCI) for critical reading of the manuscript; L. van Deemter (NKI) for expert help with generating mouse tumor lines; and M. Yao (CINJ), S. Landini (DFCI), and E. Briggs (DFCI) for expert technical help. We also thank J. Lee for providing a murine *Xist* plasmid. D.P.S. wishes to acknowledge funding from the Robert and Deborah First Family Foundation, S.D.D. from an NSF-NATO Postdoctoral Research Fellowship, J.F. from ARC, S.R. from the Swiss National Science Foundation and the Schweizerische Stiftung für medizinisch-biologische Stipendien, X.L. and J.J. from the Dutch Cancer Society, S.G. from the NIH and the UMDNJ Foundation, and D.M.L. from the National Cancer Institute. D.M.L. is a research grantee of and scientific consultant to the Novartis Institute for Biomedical Research.

Received: March 2, 2006

Revised: October 30, 2006

Accepted: February 21, 2007

Published: March 8, 2007

REFERENCES

- Ausubel, F.M., Brent, R., Kingston, R.E., Moore, D.D., Seidman, J.G., Smith, J.A., and Struhl, K. (1999). *Short Protocols in Molecular Biology* (New York: John Wiley & Sons).
- Boulton, S.J., Martin, J.S., Polanowska, J., Hill, D.E., Gartner, A., and Vidal, M. (2004). BRCA1/BARD1 orthologs required for DNA repair in *Caenorhabditis elegans*. *Curr. Biol.* *14*, 33–39.
- Brodie, S.G., and Deng, C.X. (2001). BRCA1-associated tumorigenesis: what have we learned from knockout mice? *Trends Genet.* *17*, S18–S22.
- Chadwick, B.P., and Lane, T.F. (2005). BRCA1 associates with the inactive X chromosome in late S-phase, coupled with transient H2AX phosphorylation. *Chromosoma* *114*, 432–439.
- Chadwick, B.P., and Willard, H.F. (2004). Multiple spatially distinct types of facultative heterochromatin on the human inactive X chromosome. *Proc. Natl. Acad. Sci. USA* *101*, 17450–17455.
- Chappuis, P.O., Nethercot, V., and Foulkes, W.D. (2000). Clinico-pathological characteristics of BRCA1- and BRCA2-related breast cancer. *Semin. Surg. Oncol.* *18*, 287–295.
- Clark-Knowles, K.V., Garson, K., Jonkers, J., and Vanderhyden, B.C. (2007). Conditional inactivation of *Brca1* in the mouse ovarian surface epithelium results in an increase in preneoplastic changes. *Exp. Cell Res.* *313*, 133–145.
- Clemson, C.M., McNeil, J.A., Willard, H.F., and Lawrence, J.B. (1996). XIST RNA paints the inactive X chromosome at interphase: evidence for a novel RNA involved in nuclear/chromosome structure. *J. Cell Biol.* *132*, 259–275.
- Diaz-Perez, S.V., Ferguson, D.O., Wang, C., Csankovszki, G., Wang, C., Tsai, S.C., Dutta, D., Perez, V., Kim, S., Eller, C.D., et al. (2006). A deletion at the mouse *Xist* gene exposes trans-effects that alter the heterochromatin of the inactive X chromosome and the replication time and DNA stability of both X chromosomes. *Genetics* *174*, 1115–1133.
- Elstrodt, F., Hollestelle, A., Nagel, J.H., Gorin, M., Wasielewski, M., van den Ouweland, A., Merajver, S.D., Ethier, S.P., and Schutte, M. (2006). BRCA1 mutation analysis of 41 human breast cancer cell lines reveals three new deleterious mutants. *Cancer Res.* *66*, 41–45.
- Ganesan, S., Silver, D.P., Greenberg, R.A., Avni, D., Drapkin, R., Miron, A., Mok, S.C., Randrianarison, V., Brodie, S., Salstrom, J., et al. (2002). BRCA1 supports *XIST* RNA concentration on the inactive X chromosome. *Cell* *111*, 393–405.
- Gudmundsdottir, K., and Ashworth, A. (2006). The roles of BRCA1 and BRCA2 and associated proteins in the maintenance of genomic stability. *Oncogene* *25*, 5864–5874.
- Huber, L.J., Yang, T.W., Sarkisian, C.J., Master, S.R., Deng, C.X., and Chodosh, L.A. (2001). Impaired DNA damage response in cells expressing an exon 11-deleted murine *Brca1* variant that localizes to nuclear foci. *Mol. Cell Biol.* *21*, 4005–4015.
- Johannsson, O.T., Staff, S., Vallon-Christersson, J., Kytola, S., Gudjonsson, T., Rennstam, K., Hedenfalk, I.A., Adeyinka, A., Kjellen, E., Wennerberg, J., et al. (2003). Characterization of a novel breast carcinoma xenograft and cell line derived from a BRCA1 germ-line mutation carrier. *Lab. Invest.* *83*, 387–396.
- Jonkers, J., Meuwissen, R., van der Gulden, H., Peterse, H., van der Valk, M., and Berns, A. (2001). Synergistic tumor suppressor activity of BRCA2 and p53 in a conditional mouse model for breast cancer. *Nat. Genet.* *29*, 418–425.
- Joukov, V., Groen, A.C., Prokhorova, T., Gerson, R., White, E., Rodriguez, A., Walter, J.C., and Livingston, D.M. (2006). The BRCA1/BARD1 heterodimer modulates ran-dependent mitotic spindle assembly. *Cell* *127*, 539–552.
- Korenberg, J.R., Chen, X.N., Devon, K.L., Noya, D., Oster-Granite, M.L., and Birren, B.W. (1999). Mouse molecular cytogenetic resource: 157 BACs link the chromosomal and genetic maps. *Genome Res.* *9*, 514–523.
- Lacroix, M., and Leclercq, G. (2005). The “portrait” of hereditary breast cancer. *Breast Cancer Res. Treat.* *89*, 297–304.
- Lee, J.T., and Jaenisch, R. (1997). Long-range cis effects of ectopic X-inactivation centres on a mouse autosome. *Nature* *386*, 275–279.
- Lin, S.C., Lee, K.F., Nikitin, A.Y., Hilsenbeck, S.G., Cardiff, R.D., Li, A., Kang, K.W., Frank, S.A., Lee, W.H., and Lee, E.Y. (2004). Somatic mutation of p53 leads to estrogen receptor alpha-positive and -negative mouse mammary tumors with high frequency of metastasis. *Cancer Res.* *64*, 3525–3532.
- Ludwig, T., Chapman, D.L., Papaioannou, V.E., and Efstratiadis, A. (1997). Targeted mutations of breast cancer susceptibility gene homologs in mice: lethal phenotypes of *Brca1*, *Brca2*, *Brca1/Brca2*, *Brca1/p53*, and *Brca2/p53* nullizygous embryos. *Genes Dev.* *11*, 1226–1241.
- Ouyang, Y., Salstrom, J., Diaz-Perez, S., Nahas, S., Matsuno, Y., Dawson, D., Teitell, M.A., Horvath, S., Riggs, A.D., Gatti, R.A., et al. (2005). Inhibition of *Atm* and/or *Atr* disrupts gene silencing on the inactive X chromosome. *Biochem. Biophys. Res. Commun.* *337*, 875–880.
- Pageau, G.J., and Lawrence, J.B. (2006). BRCA1 foci in normal S-phase nuclei are linked to interphase centromeres and replication of pericentric heterochromatin. *J. Cell Biol.* *175*, 693–701.
- Pageau, G.J., Hall, L.L., and Lawrence, J.B. (2006). BRCA1 does not paint the inactive X to localize XIST RNA but may contribute to broad changes in cancer that impact XIST and Xi heterochromatin. *J. Cell. Biochem.*, in press. Published online December 4, 2006. 10.1002/jcb.21188.
- Parvin, J.D., and Sankaran, S. (2006). The BRCA1 E3 ubiquitin ligase controls centrosome dynamics. *Cell Cycle* *5*, 1946–1950.
- Patel, K.J., Yu, V.P., Lee, H., Corcoran, A., Thistlethwaite, F.C., Evans, M.J., Colledge, W.H., Friedman, L.S., Ponder, B.A., and Venkitaraman, A.R. (1998). Involvement of *Brca2* in DNA repair. *Mol. Cell* *1*, 347–357.
- Richardson, A.L., Wang, Z.C., De Nicolò, A., Lu, X., Brown, M., Miron, A., Liao, X., Iglehart, J.D., Livingston, D.M., and Ganesan, S. (2006). X chromosomal abnormalities in basal-like human breast cancer. *Cancer Cell* *9*, 121–132.
- Scully, R., Chen, J., Plug, A., Xiao, Y., Weaver, D., Feunteun, J., Ashley, T., and Livingston, D.M. (1997). Association of BRCA1 with Rad51 in mitotic and meiotic cells. *Cell* *88*, 265–275.

Shen, S.X., Weaver, Z., Xu, X., Li, C., Weinstein, M., Chen, L., Guan, X.Y., Ried, T., and Deng, C.X. (1998). A targeted disruption of the murine *Brca1* gene causes gamma-irradiation hypersensitivity and genetic instability. *Oncogene* 17, 3115–3124.

Silver, D.P., and Livingston, D.M. (2001). Self-excising retroviral vectors encoding the Cre recombinase overcome Cre-mediated cellular toxicity. *Mol. Cell* 8, 233–243.

Soriano, P. (1999). Generalized lacZ expression with the ROSA26 Cre reporter strain. *Nat. Genet.* 21, 70–71.

Sorlie, T., Tibshirani, R., Parker, J., Hastie, T., Marron, J.S., Nobel, A., Deng, S., Johnsen, H., Pesich, R., Geisler, S., et al. (2003). Repeated observation of breast tumor subtypes in independent gene expression data sets. *Proc. Natl. Acad. Sci. USA* 100, 8418–8423.

Turner, N., Tutt, A., and Ashworth, A. (2004). Hallmarks of 'BRCAness' in sporadic cancers. *Nat. Rev. Cancer* 4, 814–819.

Xiao, C., Sharp, J.A., Kawahara, M., Davalos, A.R., Difilippantonio, M.J., Hu, Y., Li, W., Cao, L., Buetow, K., Ried, T., et al. (2007). The *XIST* noncoding RNA functions independently of BRCA1 in X inactivation. *Cell* 128, this issue, 977–989.

Xu, X., Weaver, Z., Linke, S.P., Li, C., Gotay, J., Wang, X.W., Harris, C.C., Ried, T., and Deng, C.X. (1999). Centrosome amplification and a defective G2-M cell cycle checkpoint induce genetic instability in BRCA1 exon 11 isoform-deficient cells. *Mol. Cell* 3, 389–395.

Xu, X., Qiao, W., Linke, S.P., Cao, L., Li, W.M., Furth, P.A., Harris, C.C., and Deng, C.X. (2001). Genetic interactions between tumor suppressors *Brca1* and *p53* in apoptosis, cell cycle and tumorigenesis. *Nat. Genet.* 28, 266–271.